Ceramics based on titanium nitride and silicon nitride sintered by SPS-method

A A Sivkov[1], D Yu Gerasimov[1] and A A Evdokimov[1]
[1]Russia, Tomsk, Lenin ave, 30, National Research Tomsk Polytechnic University

e-mail: kraamis@gmail.com

Abstract. The dependences of the microstructure and physical and mechanical properties of ceramic mixtures Si_3N_4/TiN in the full range of mass ratios of the components. Was also investigated directly, and the process of sintering occurring during a physical or chemical processes, in particular, has been obtained and the hardness of the material density on the ratio of the conductive titanium nitride phase and a silicon nitride insulating phase with values above and below the percolation threshold. Also obtained was pure ceramics based on titanium nitride with high physical-mechanical characteristics (H = 21.5 GPa).

1. Introduction

Today, there is a high demand for metal-cutting tools, created from light ceramic materials with relatively high hardness [1]. These materials are in demand in various industries. Oxygen-free ceramic based on silicon nitride is quite popular due to its high chemical resistance, high temperature resistance and dielectric properties [2, 3]. However, this ceramics has a number of disadvantages, in particular, silicon nitride is an insulator and therefore it is unacceptable for spark plasma sintering (SPS). In fact, for pure silicon nitride, this process is similar to the hot isostatic pressing. This problem can be solved by various ways, in particular, by doping the silicon nitride with small additions of oxides (aluminum oxide Al_2O_3 and yttrium oxide Y_2O_3) in an amount of 10-12% [4-8]. However, the disadvantage of this method is the clogging of the ceramics sample with silica and aluminum. This can lead to decreasing in physical and mechanical properties of the sample due to the appearance of local dense centers.

TiN is often used as the doping agent in the preparation of metal-cutting samples [4-6]. TiN is selected because of its high electrical conductivity, which allows increasing the sinterability of Si_3N_4, without a strong fall in strength characteristics [1, 7, 8]. Also, TiN has a high melting point, good hardness, chemical, tribological and corrosion resistance.

SPS is a relatively new method for consolidating nanocomposites in high-speed process, and this method is highly effective for obtaining nanocomposites in a short time. In previously published literature it was observed that nanostructured ceramics with high physical-mechanical characteristics based on Si_3N_4/TiN can be obtained after a short preparation of raw powder with following sintering [9, 10].

The aim of this work is to consider the use of titanium nitride simultaneously in two roles: as a doping factor at low levels, and as a component of the composition at a concentration above the percolation threshold. Spark plasma sintering method is chosen because of its advantages over the two-step methods. In particular, using this technology large recrystallizing ceramics grains can be avoided both with maintaining nanostructures.

2. Experimental

Pure silicon nitride nanopowders [10-25 nm, SSA=60m^2/g, α/(α+β)=50%, X-ray amorphous phase] and titanium nitride produced by using the system based on coaxial magneto plasma accelerator [11-17] [TiN - 90%, αTi - 10%] were used for sintering.

Five types of powder blanks were prepared and their types are indicated in Table 1.

Table 1. The content of titanium nitride and silicon in experiments.

Experiment	1	2	3	4	5
TiN / Si$_3$N$_4$, %	100 / 0	75 / 25	50 / 50	25 / 75	0 / 100

The required weight of the powder was weighed using high-precision electronic scales, to the nearest hundredth of a gram. Further the mixed powder compositions were subjected to thorough mixing, activating, and deagglomerating in planetary mill for one hour. The process was carried out with using steel grinding balls.

Significant increase in bulk density from 0.06 g/cm^3 to 0.48 g/cm^3 for pure Si$_3$N$_4$, and from 0.18 g/cm^3 to 0, 6 g/cm^3 for pure TiN is attributed to important results of such preparation.

Sintering was performed by SPS bot in helium at 1 atmosphere pressure and under vacuum at 1300°C. Other sintering conditions were the same and as follows: the heat rate V_T = 100°C/min, the pressing force P=60 MPa (~ 20 kN) and the exposure absence with a constant temperature. The material was placed into a graphite mold with an inside diameter of 20 mm.

After sintering the samples were cleaned, ground and polished using special machine. The sample hardness was studied by microhardness measuring using a Vickers indenter at a load of 1 kg for 10 seconds. Determination of hardness was performed by the method of unrestored print. The microstructure was investigated by scanning electron microscopy on a polished surface of the untreated and cleaved sample. Phase composition was determined by X-ray diffraction.

3. Results and discussion

Table 2 shows the results of XRD analysis for powder samples and ceramics materials, obtained in a series of experiments, conducted at the sintering temperature 1300°C. This range has been chosen as a basis, because of the critical temperature for titanium nitride is 1450°C and at this temperature TiN begins to react with the carbon from which the mold is made.

The divergence in XRD analysis data with the original data on the composition (Table 1) can be explained by the following factors: firstly, the grinding time was enough for partial mechanosynthesis of titanium nitride; secondly, the presence of amorphous phase in silicon nitride shifts the equilibrium phases in the direction of titanium nitride. The presence titanium suboxides (sample 1), appearing after sintering, can be explained by oxidation of free titanium either during reacting with oxygen in the chamber or after removal of the sample and cooling it in the open air. Also in experiments 3 and 4, free silicon appeared. This fact can be explained by the growth of silicon grains due to pressure load.

Also in experiments 2, 3 and 4 there is a presence of such titanium silicide as TiSi$_2$ and Ti$_5$Si$_3$. The high concentration of silicide in the experiment 2 is explained by both the high content of titanium metal in the sample and the presence of free silicon. When heating the powder sample by pulse current during the SPS the differences in current between the sample and the mold are determined by the conductivity of the powder sample. Due to the small process time (up to 20 minutes) the system does not have time to warm up evenly and there is heterogeneity in the distribution of temperature. It leads to the fact that the formation of titanium silicide is directly determined by the conductivity of the sample. The transition of the silicon nitride from α-phase to β-phase does not occur due to insufficient temperature. There was also no transition from β-phase and γ-phase due to low pressure molding.

Figure 1 shows the curves of the SPS- process, such as temperature, pressure, current and sealing. The temperature curve is removed by the thermometer from the outside of the graphite mold. The constant temperature level at the beginning and end of the process is due to the physical limitations of the pyrometer, the temperature begins to register from the value 467°C. It should also be noted that the

temperature inside the sample is above then the outside one, the difference can be up to 100-120°C [18].

Table 2. Results of X-ray diffraction analysis of the powder materials and ceramic samples.

Phase	%	CSR, нм	Phase	%	CSR, нм
*** powder 1 ***			*** ceramic 1 ***		
cTiN	90	--	cTiN	90	--
αTi	10	15	αTi	5	59.54
----	----	----	Ti_xO_y	5	--
*** powder 2 ***			*** ceramic 2 ***		
cTiN	73	--	cTiN	69	--
αTi	7	17	$TiSi_2$ / Ti_5Si_3	7 / 17	27 / 63
α/β Si_3N_4	3 / 17	41 / 12	α/β Si_3N_4	3 / 3	23 / 24
*** powder 3 ***			*** ceramic 3 ***		
cTiN	71	--	cTiN	72	46
αTi	7	12	$TiSi_2$ / Ti_5Si_3	3 / 1	12 / 22
α/β Si_3N_4	6 / 16	62 / 56	α/β Si_3N_4	10 / 10	35 / 48
----	----	----	aSi	3	49
*** powder 4 ***			*** ceramic 4 ***		
cTiN	38	--	cTiN	47	49
αTi	1	111	$TiSi_2$ / Ti_5Si_3	2 / 2	13 / 34
α/β Si_3N_4	25 / 36	92 / 51	α/β Si_3N_4	26 / 20	43 / 23
----	-----	----	aSi	3	70
*** powder 5 ***			*** ceramic 5 ***		
α/β Si_3N_4	55 / 45	47 / 53	α/β Si_3N_4	50 / 50	38 / 52

The main curves in the figure are the sealing curves. In every case, the sealing is substantially different. For a pure titanium nitride pre sealing on the step of pressure growth (t_0-t_1) does not occur because the titanium nitride powder has a fairly rigid structure (as shown below) and there is no possibility to further increase in the bulk density before sintering. Further, at step t_1-t_2 when the powder is impacted only with pressure over an extended period of time ~250-270 seconds, the partial seal occurs that is similar to the process of cold isostatic pressing. At this stage, the heating does not occur, because of the sample temperature is below the soft threshold pyrometer (467°C) and the current switching point (600°C). The third stage (t_2-t_3) is characterized by uncontrolled temperature growth due to increasing heating current. During130-150 seconds the temperature rises up to 600°C. After that the speed is normalized and reduced to a predetermined program values. At this point, it is possible to see a small decompression due to thermal expansion exceeding hydraulic compression. Further, at t_3-t_4 there is a controlled heating of the sample at a constant pressing force. Sealing curve knee can be explained due to the fact that the processes of liquid-phase sintering on the grain boundaries begin to prevail over the processes of thermal expansion. It leads to increasing density of the sample at this stage. At the time t_4 the heating current is switched off and the sample begins to cool down both by radiation and by convection processes in the atmosphere of helium. At the time t_5 the compaction pressure reduction begins. There is no matter substantially sealing at this stage because of the lack of sealing factors.

As for the second sample, consisting of equal mass fractions of titanium nitride and silicon nitride, it should be noted that the above processes description is applicable in this case, but with some additives. The partial compaction during stages t_1-t_2 and t_2-t_3 is observed to a much lesser degree than for a pure titanium nitride. This is because of the mixture conductivity is far less than the conductivity of pure titanium nitride, and liquid-phase processes occur at the grain boundaries are much less active.

However, due to decreasing Joule heating, the nature of seal and decompaction in the area around t_3-t_4 is similar to the sample made of pure titanium nitride with a slightly lower seal. Also in the sample there is the presence of free silicon particles, which rose above the limit of X-rays, as mentioned above. It also fits in a sealing scheme, which depends on the composition of the sample.
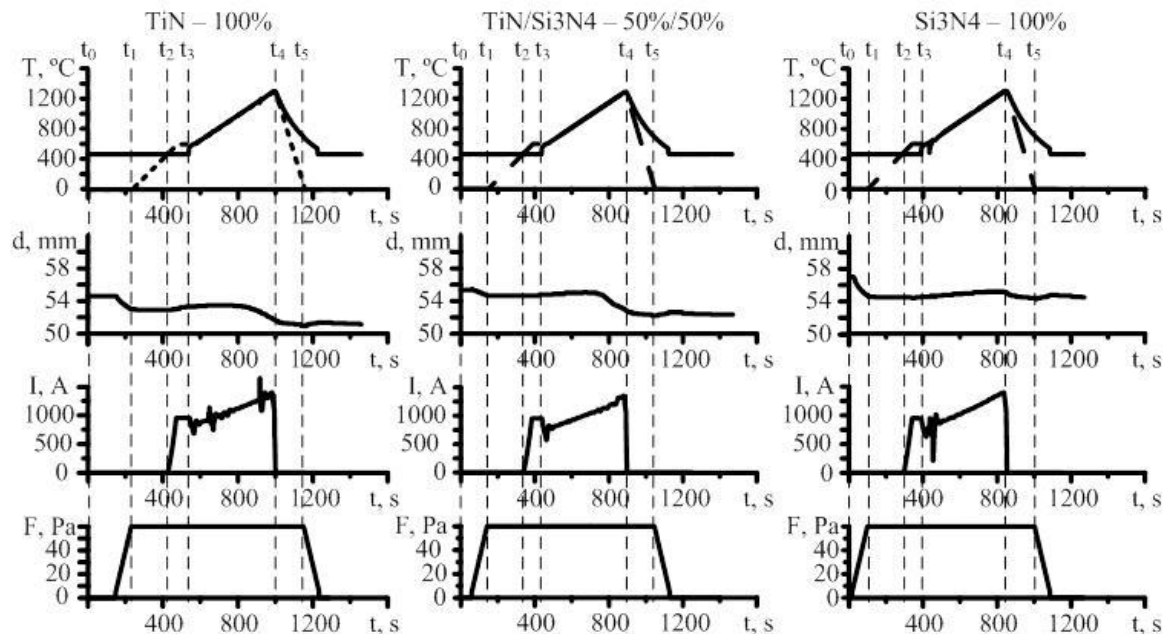

Figure 1. The process parameters for the spark plasma sintering (experiments 1, 3, 5).

For the third sample, consisting of pure silicon nitride, the spark plasma sintering process differs significantly. This is due to the fact that the sample is below the percolation threshold [4], and its conductivity is lower by orders of magnitude than that of the previous samples. In step t_0-t_1 there is a sharp seal due to applying large force to the sample. The titanium nitride matrix is absent in the sample, and the sample has almost no resistance to the primary compression. The sample relatively quick condenses almost to the end value. During several steps from t_1 to t_4 there is some decompaction that can be explained by the fact that there is no liquid phase process. Thus the Joule heating process dominates. The seal during the cooling step is also explained by thermal contraction.

Table 3 and Figure 2 show the mechanical testing data for the samples sintered at 1300°C. The figure 2 also clearly shows two abrupt changes of hardness. These data can be explained by a significant difference between the conductivity of titanium nitride (conductor) and silicon nitride (dielectric). The low hardness at low TiN contents (experiments 4 and 5) can be explained by the fact that the content of the conductive fraction is below the percolation threshold. When the threshold is exceeded, equal to 30%for a given pair of substances [4], both the conductivity and the sinterability sharply increase. The second hardness surge occurs when there is no dielectric fraction (exp. 1).
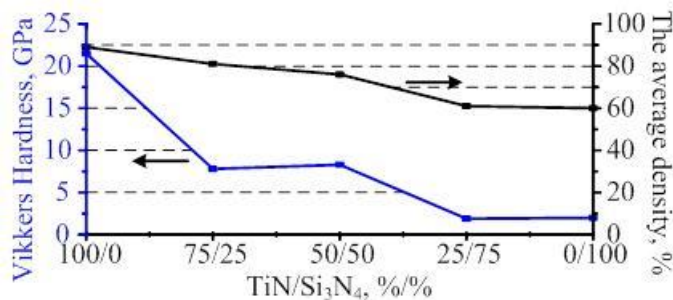

Figure 2. Curves of density and hardness for the ceramic samples, in dependence on the phase ratio of titanium and silicon nitride, sintered by spark plasma sintering in the helium environment at a temperature of 1300°C, with heating speed rate of 100°C/min without time delay, and a compression pressure 60 GPa.

Similar abrupt changes are also clearly visible in the density curve, which can also be explained by a sharp change in conductivity samples.

Figure 3 shows SEM images of the samples sintered at a temperature 1300°C with different ratios of titanium and silicon nitride. Series a (a1-a3) shows feedstock surface and chipping of the ceramics sintered from pure titanium nitride. Series b (b1-b3) is for mix of titanium nitride and silicon nitride in equal amounts. Series c) (c1-c3) is for pure silicon nitride.

Table 3. Data of the density and hardness for the ceramic samples, in dependence on the phase ratio of titanium and silicon nitride, sintered by spark plasma sintering in the helium environment at a temperature of 1300°C, with heating speed rate of 100°C/min without time delay, and a compression pressure 60 GPa.

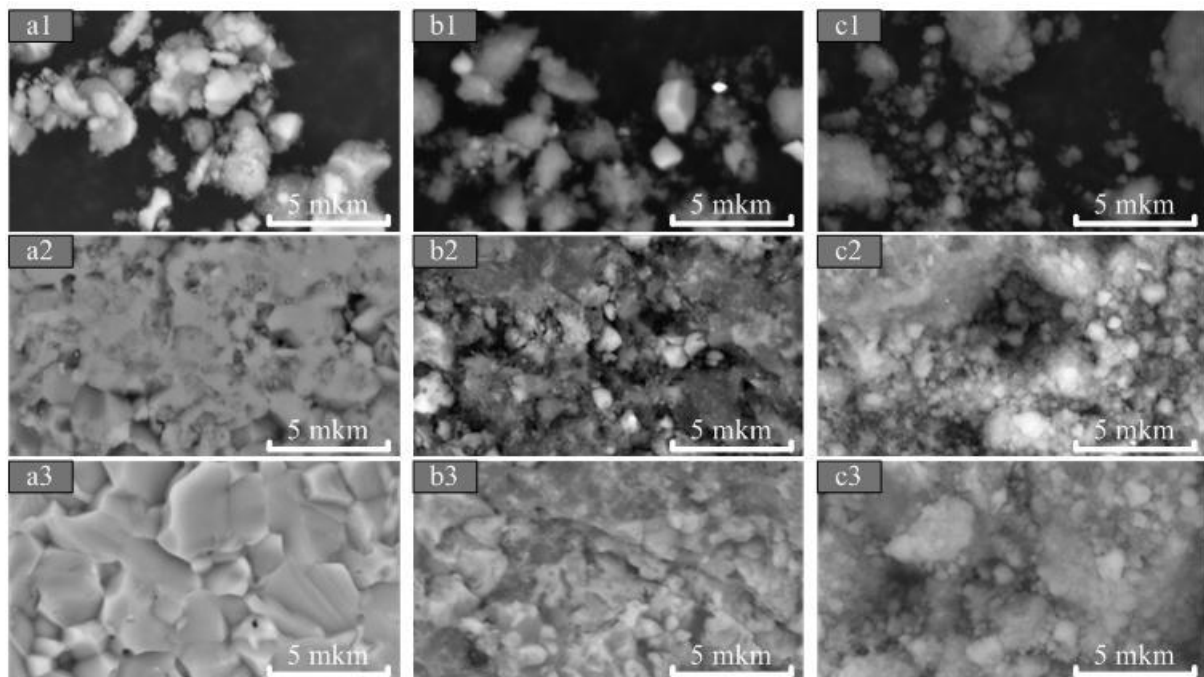| Experiment	Structure		Ceramic	
	TiN, %	Si_3N_4, %	Density, g/cm^3 (%)	Hardness, GPa
1	100	0	4.84 (89%)	21.5
2	75	25	3.82 (81%)	7.8
3	50	50	3.21 (76%)	8.3
4	25	75	2.30 (61%)	1.9
5	0	100	2.05 (60%)	2.0

Figure 3. SEM-microscopy data for ceramics sintered by spark plasma sintering at 1300°C. Column A) TiN - 100% (Experiment 1, Table 1), b) TiN/Si_3N_4 - 50%/50% (Experiment 3, Table 1), c) Si_3N_4 - 100% (Experiment 5, Table 1). Rows: 1) ultrafine feedstock after machining, 2) SEM-picture of polished sample surface, 3) SEM-picture of raw chipping of the sample.

In line 1 the powdered materials, treated in a planetary mill directly before sintering, are shown. Titanium nitride particles have strict faceted structure and a darker color. It is seen that the range of particle size distribution is quite wide, from a few microns to less than 100 nm nanoparticles. Silicon nitride has a cotton-like structure due to its high dispersion and availability of silicon in the form of fine amorphous phase. Due to the high dispersion, silicon nitride has a high tendency to agglomerate, gathering in agglomerates with a size of several microns. In consequence of the fact that after

activating on the planetary mill, the bulk density dramatically increases, it leads to an increasing the individual agglomerates and expanding the particle size distribution.

In line 2 SEM-images of the polished surface of the sintered samples are shown. Here it is possible to see the grain structure with a clear division into components. Moreover, according to data of sintering for all samples, there is no significant particle growth of both titanium nitride and silicon nitride due to insufficiency of this temperature for the grain growth of both titanium nitride and silicon nitride [4]. It can be seen in more details on the raw chipping of the samples (line 3). Also the wide range of size distribution is more a plus than a minus, because the smaller particles fill the pores between large ones, thereby achieving high packing density of particles.

Conclusion

In this work, the study is carried out to obtain ceramics based on titanium nitride and silicon nitride by spark plasma sintering. There is information about the processes occurring during sintering, in particular, about the formation of by-products from the impurities in the starting components. Also there is information about the dependence of the density and hardness on the ratio of the components and their electrical conductivity. Also the pure ceramics based on titanium nitride with high physical-mechanical characteristics (H = 21.5 GPa) is obtained.

Acknowledgment

References
[1]   Lee C, Lu H, Wang C, Nayak P and Huang J 2010 *Journal of alloys and compounds* **508** 2
[2]   Gogotsi Y 1994 *Journal of Materials Science* **29** 2541
[3]   Huang J, Chen S and Lee M 1994 *Journal of Materials Research* **9** 2349
[4]   Guo Z, Blugan G, Kirchner R, Reece M, Graule T and Kuebler J 2007 *Ceramics International* **33** 1223
[5]   Chunyan T, Hai J and Ning L 2011 *International Journal of Refractory Metals and Hard Materials* **29** 14
[6]   Liu C and Huang J 2003 *Ceramics International* **29** 679
[7]   Yoshimura M, Komura O and Yamakawa A 2001 *Scripta Materialia* **44** 1517
[8]   Gao L, Li J, Kusunose T and Niihara K 2004 *Journal of the European Ceramic Society* **24** 381
[9]   Tokita M 2004 *Journal of Material Science* **5** 78.
[10] Ayas E, Kara A and Kara F 2008 *Journal of the Ceramic Society of Japan* **116** 812
[11] Evdokimov A, Sivkov A, Gerasimov D, Saigash A and Khasanov A. 2013 *Russian Physics Journal* **55** 983
[12] Sivkov A, Gerasimov D and Evdokimov A 2014 *Instruments and Experimental Techniques* **57** 222
[13] Sivkov A, Gerasimov D, Saigash and Evdokimov A 2012 *Russian Physics Journal* **54** 1160
[14] Sivkov A, Gerasimov D, Saigash A and Evdokimov A 2012 *Russian Electrical Engineering* **83** 39
[15] Pak A, Sivkov A, Shanenkov I, Rahmatullin I and Shatrova K 2015 *Int. J. Refract. Met. Hard Mater.* **48** 51
[16] Shanenkov I I, Pak A Ya, Sivkov A A and Shanenkova Yu L 2014 *MATEC Web of Conferences* **19** 01030
[17] Sivkov A, Saygash A, Kolganova J and Shanenkov I 2014 *IOP Conf. Series Mater. Sci. Eng.* **66** 012048
[18] Wan J, Duan R and Mukherjee A. 2005 *Scripta Materialia* **53** 663.